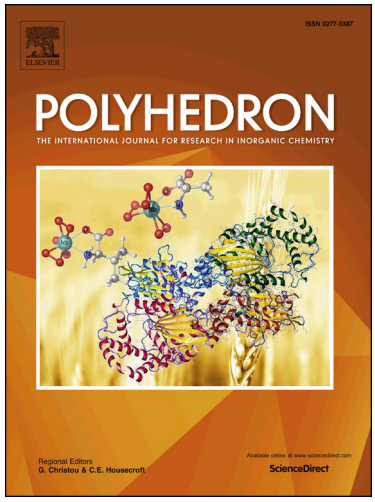

A zig-zag end-to-end azido bridged Mn^{III} 1-D coordination polymer: Spectral elucidation, magnetism, redox study and biological activity

Kuheli Das, Amitabha Datta, Belete B. Beyene, Chiara Massera, Eugenio Garribba, Chittaranjan Sinha, Takashiro Akitsu, Shinnosuke Tanka

PII: S0277-5387(17)30127-4
DOI: http://dx.doi.org/10.1016/j.poly.2017.02.017
Reference: POLY 12484

To appear in: *Polyhedron*

Received Date: 21 December 2016
Revised Date: 10 February 2017
Accepted Date: 12 February 2017

Please cite this article as: K. Das, A. Datta, B.B. Beyene, C. Massera, E. Garribba, C. Sinha, T. Akitsu, S. Tanka, A zig-zag end-to-end azido bridged Mn^{III} 1-D coordination polymer: Spectral elucidation, magnetism, redox study and biological activity, *Polyhedron* (2017), doi: http://dx.doi.org/10.1016/j.poly.2017.02.017

A zig-zag end-to-end azido bridged Mn^{III} 1-D coordination polymer: Spectral elucidation, magnetism, redox study and biological activity

Kuheli Das[a,b], Amitabha Datta[a,b,*], Belete B. Beyene[a], Chiara Massera[c], Eugenio Garribba[d], Chittaranjan Sinha[b,*], Takashiro Akitsu[e], Shinnosuke Tanka[e]

[a]*Institute of Chemistry, Academia Sinica, Nankang – 105, Taipei, Taiwan*

[b]*Department of Chemistry, Jadavpur University, Kolkata – 700032, India*

[c]*Dipartimento di Chimica, Universita` degli Studi di Parma, Viale delle Scienze, 17/A, 43124 Parma, Italy*

[d]*Dipartimento di Chimica e Farmacia, Università di Sassari, Via Vienna 2, I-07100 Sassari, Italy*

[e]*Department of Chemistry, Faculty of Science, Tokyo University of Science, 1-3 Kagurazaka, Shinjuku-ku, Tokyo 162-8601, Japan*

*Corresponding authors. amitd_ju@yahoo.co.in (A. Datta); c_r_sinha@ yahoo.com (C. Sinha)

A B S T R A C T

A zig-zag one-dimensional Mn(III) coordination polymer, $\{[C_6H_4(O)CHN(CH_2)_2NCH(O)C_6H_4]Mn(N_3)\}_n$ (**1**) has been synthesized reacting a manganese salt with the Schiff base precursor H_2L, obtained condensing salicyldehyde and ethylenediamine. The compound has been characterized by IR, UV-vis and EPR spectroscopy. Single crystal X-ray diffraction studies have revealed that the Mn atom possesses a distorted octahedral environment and the metals connected by end-to-end azido lignads lead to the formation of 1-D zig-zag molecular chains. Temperature dependent magnetic studies have shown the presence of weak anti-ferromagnetic coupling among the Mn centers. Cyclic voltammetry has evidenced the presence of a reversible redox couple for the Mn^{3+}/Mn^{2+} system. Both the ligand and complex **1** exhibit anti-mycobacterial activity and considerable efficacy on *M. tuberculosis* H37Rv ATCC 27294 and *M. tuberculosis* H37Ra ATCC 25177 strains. The cytotoxicity study on different human cancer cell lines (Caco 2, MCF7 and A549) suggests that complex **1** has potential anticancer properties.

Keywords: Mn(III); Coordination polymer; Spectra; Cyclic voltammetry; Biological property

1. Introduction

The rational design and synthesis of novel coordination compounds based on transition metals and multifunctional bridging ligands is of great research interest, due to their interesting frameworks and potential applications as functional materials. Schiff base metal complexes are very important tools for inorganic chemists as they are widely used in constructing supramolecular architectures such as coordination polymers or double and triple helicates [1,2]. Additionally, they can be employed in a variety of applications, for instance as antibacterial and antifungal agents [3], in homogeneous or heterogeneous catalysis [4-7] and magnetism [8]. There are numerous accounts in the literature describing the chemistry of metal complexes of Schiff base ligands containing two, three, four, five and six donor atoms [9]. Multidentate Schiff bases with NO donor atoms have been often used to block the coordination sites of metal ions which prefer square planar or square pyramidal geometry and to saturate the coordination number of the metal ion. A bridging ligand has been used to synthesize multinuclear metal complexes [10-13]. The nature and the tuning of magnetic interactions between metal centres are crucial points in the conception of molecule-based magnetic materials [14-18]. The manganese(III) salen-type compounds are generally in equilibrium between the monomeric and the dimeric species, their solid state form depending on the steric characteristics of the

salen-type Schiff bases [14]. Dimeric manganeses(III) complexes generally exhibit an antiferromagnetic intra-dimer interaction which is very well explored [19-23], but a few examples of ferromagnetic interactions have been reported as well [24-27]. Pseudohalide coligands, such as cyanide, azide, thiocyanate, and dicyanamide (dca), have been utilized to bridge transition metal–Schiff base complexes, in order to explore and modify their magnetic properties and network topology, as well as to increase the dimensionality of the resulting coordination polymers [28-30]. Magnetic interactions between the metal centers of such complexes can be tuned by skillful control of the chain length and the byte angle of the bridging ligands, and in this respect the azide ion plays a significant role. The different binding modes of the azide ion are shown in **Scheme 1**. The end-to-end or 1,3-coordination mode of N_3^- generally results in antiferromagnetic coupling between the metal centres but if the bond angle in M-$\mu_{1,3}$-N_3-M is very large, then the sign of the coupling may be reversed [31-37]. In contrast, the end-on or 1,1-coordination mode produces ferromagnetic coupling, but the ferromagnetic ordering between the metal centers is reduced if the bridging byte angle exceeds 108° [38]. Tuberculosis, which is caused primarily by *Mycobacterium tuberculosis* and rarely by *M. bovis* and *M. africanum*, is one of the oldest disease in the world affecting lungs and spreading to the other organs [39]. At present, a million children per year has died from this disease [40]. Mycobacteria

resist to many chemicals, disinfectant antibiotics and chemotherapeutical agents [41,42]. Mycobacteria show a strong resistance to most of the antibiotics and chemicals due to the low permeability of the mycobacterial cell wall. Porins in the thickness and low permeability of this bilayer membrane allow inefficient permeability of the substances [42]. The prospect of developing new and affective drugs is central to the global control of tuberculosis. As an extension of earlier work, we report one zig-zag end-to-end azido bridged Mn(III) 1-D coordination polymer $\{[H_2L]Mn(N_3)\}_n$ (**1**), where H_2L = $C_6H_4(OH)CH{=}N\text{-}CH_2CH_2\text{-}N{=}CH(OH)C_6H_4$. We have systematically characterized the compound by X-ray diffraction spectrometry, as well as by IR and UV-vis studies. Temperature and solvent dependent EPR spectra have been also obtained and discussed. Besides studying the magnetic and cyclic voltammetric properties, we have also focused our attention on the anti-mycobacterial activity on human tuberculosis cells like *M. tuberculosis* H37Rv ATCC 27294 and *M. tuberculosis* H37Ra ATCC 25177 strains.

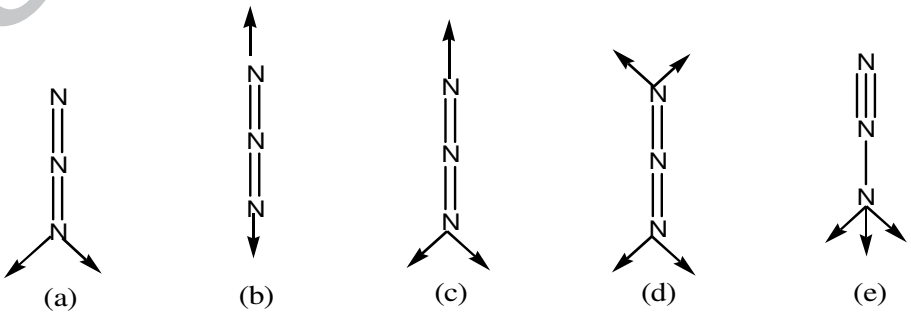

Scheme 1. Different binding modes of the azide ion.

2. Results and discussion

2.1. Description of crystal structure

The ligand, (H_2L) [$C_6H_4(OH)CH=N-CH_2CH_2-N=CH(OH)C_6H_4$] was prepared by the condensation of salicyldehyde and ethylenediamine (2:1 mole proportion) in methanol [43]. H_2L reacted with $Mn(CCl_3COO)_2.4H_2O$ in the same solvent to yield compound **1** which was crystallized by slow evaporation. Single-crystal X-ray analysis revealed that compound **1** crystallizes in the orthorhombic space group $Pca2_1$. As shown in **Figure 1**, the monomeric unit consists of one Mn ion, one ligand L^{2-} and a coordinating azide. The resulting coordination around each Mn ion is therefore octahedral; the vertexes are occupied by the azide nitrogen atoms N3 and N5a, while the equatorial plane is occupied by the atoms O1, O2, N1 and N2 of the tetradentate Schiff base ligand. In the lattice, the different chains are stabilized by C-H···N contacts.

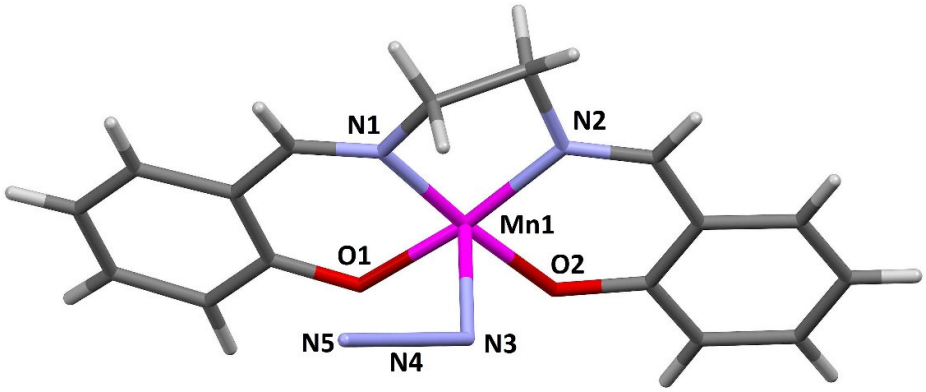

Figure 1. Molecular structure of the monomeric unit [Mn(L)(N_3)] with partial labelling scheme.

Due to Jahn-Teller effect, the Mn-N bond distances in the apical position (Mn(1)–N(3) = 2.270(7) Å and Mn(1)–N(5a) = 2.311(7) Å) are significantly longer than those in the equatorial plane (Mn(1)–O(1) = 1.895(5) Å, Mn(1)–O(2) = 1.872(5) Å and Mn(1)–N(1) = 1.976(6) Å, Mn(1) = N(2) = 1.987(6) Å) (see **Table 1**). These values are similar to those of other reported complexes with the same [MnN_4O_2] coordination sphere [44]. The basal bond angles are all close to 90° with the exception of the N(1)–Mn(1)–N(2) bite angle (81.96 (8)°) which is considerably smaller. The monomeric unit is repeated along the *b* axis of the unit cell, to yield a zig-zag polymeric chain in which the metal centers are connected through the nitrogen atoms of symmetry-related azide ligands. The one-dimensional polymeric chain in which the azide ions are coordinated in end-to-end fashion is depicted in **Figure 2**. The bridging $(N_3)^-$ anions are practically linear, with N3-N4-N5 bond angles of 179.4(5)°. One of the phenyl rings of the Schiff base

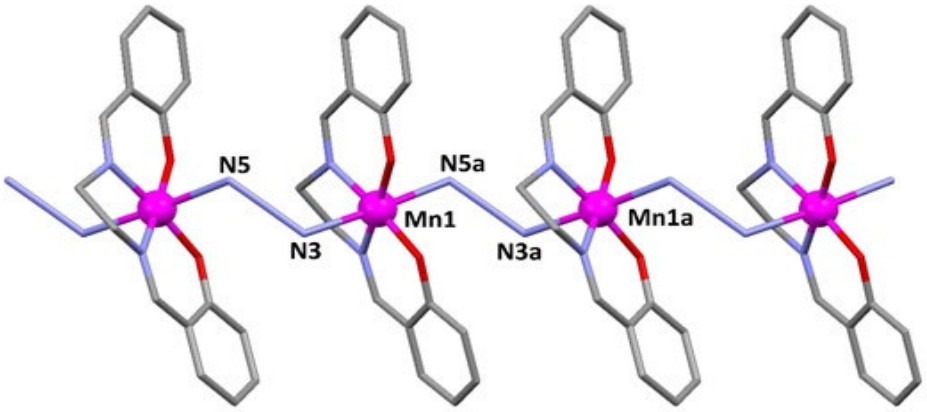

Figure 2. View of the 1D polymer along the *b* axis of the unit cell. Hydrogen atoms have been omitted for clarity. a: 1,5-x; ½+y; z.

ligand (C4–C9), (see **Figure S1** for the complete labeling scheme) is slightly twisted out of the central hydrazine moiety by the dihedral angle of 16.47° (**Figure 2**). All manganese atoms along the chain are localized in the same plane with intra-chain Mn-Mn distances of 5.535(3) Å. The shortest inter-chain metal–metal separation in the lattice is 7.120(2) Å.

Table 1. Selected geometric parameters (Å, °) for **1**.

Mn1-O1	1.895(5)	N3-Mn1-N5a	176.96(8)
Mn1-O2	1.872(5)	O1-Mn1-O2	94.02(9)
Mn1-N1	1.976(6)	N1-Mn1-N2	81.96(8)
Mn1-N2	1.987(6)	O1-Mn1-N1	92.03(9)
Mn1-N3	2.270(7)	O2-Mn2-N2	92.09(9)

Mn1-N5a	2.311(7)
Mn1•••Mn1a	5.535(3)

a: 1,5-x; ½+y; z

2.2. IR spectra

From the IR spectroscopic analysis, the strong absorption band corresponding to $\nu_{N\equiv N}$ of the azido ligand appears at 2029 cm^{-1}. The band at 1614 cm^{-1} is attributable to $\nu_{C=N}$ (imine bond) and this band shifts to a lower frequency region compared to that obtained for the respective free ligand [at 1640 cm^{-1} (H_2L)] [45]. Ligand coordination with the manganese ion is substantiated by two types of bands at 445 cm^{-1} and 361 cm^{-1}, corresponding to ν_{Mn-N} and ν_{Mn-O}, respectively.

2.3. Electronic spectra

The electronic spectra of compound **1** comprises two absorption regions. It shows low-intensity absorption bands associated with d−d transitions at around 515 (ε = 390 $mol^{-1}cm^{-1}$) nm [46]. In the case of an octahedral complex, only one such transition is expected in the form of an intense band corresponding to $^5T_{2g} - {}^5E_g$. It also displays two strong absorption bands in the region 230 (ε = 1100 $mol^{-1}cm^{-1}$) and 275 nm (ε = 1150 $mol^{-1}cm^{-1}$), which can be assigned to charge transfer from the ligand to the Mn(III) centre (LMCT).

2.4. EPR spectra

EPR spectra of the polycrystalline complex **1** were recorded at 298 and 77 K (**Figure 3**). The spectral intensity is very low and this is compatible with the oxidation state +3 of Mn in good agreement with the crystal structure. Indeed, EPR spectra of transition metal ions with an even number of unpaired electrons are very difficult to obtain, principally because the ground state spin multiplet is largely split in a zero magnetic field by the low symmetry components of the crystal field [47]. A broad and isotropic signal emerges only at highest instrumental gain (trace b of **Figure 3**), with *g* values of 2.007 ± 0.005 (298 K) and 2.005 ± 0.005 (77 K). Such unresolved signal can be attributed to a Mn(II) impurity in the structure of **1** and is due to the presence of a mixture of inter-center exchange and dipolar interactions, recently discussed by Brondino and co-workers [48]. The values of *g* are compatible with a distorted octahedral environment around Mn(III), consistent with the X-ray structure of **1** [49,50].

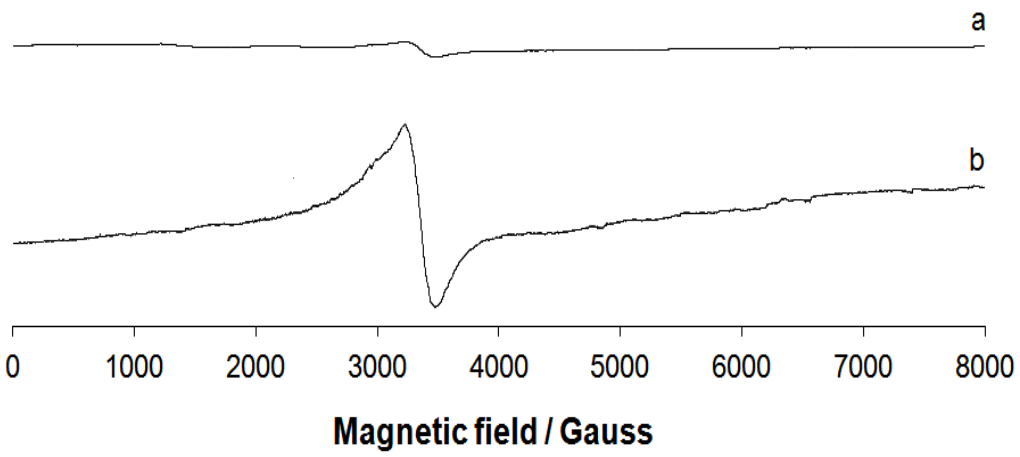

Figure 3. X-band EPR spectra recorded at 77 K on the polycrystalline complex **1**. In trace b the signal was amplified by ten times using a highest instrumental gain.

EPR spectra in solution were also recorded; complex **1** was dissolved in both non-coordinating and coordinating solvents: DMF (**Figure 4**, trace a), DMSO (**Figure 4**, trace b), MeOH (**Figure 4**, trace c) and a mixture CH_2Cl_2/toluene 60/40 v/v (**Figure 4**, trace d). The results are very similar to those obtained in the solid state and the intensity of the spectra is very low. Very week isotropic signals centered around $g \sim 2$ are detected in all the solvents and the measured g value is 2.010 ± 0.005 in DMF, 2.009 ± 0.005 in DMSO, 2.013 ± 0.005 in MeOH and 2.013 ± 0.005 in the mixture CH_2Cl_2/toluene 60/40 v/v. In this case too, these signals can be attributed to the impurities represented by Mn(II). The absence of hyperfine coupling interaction, usually observed for Mn(II) in

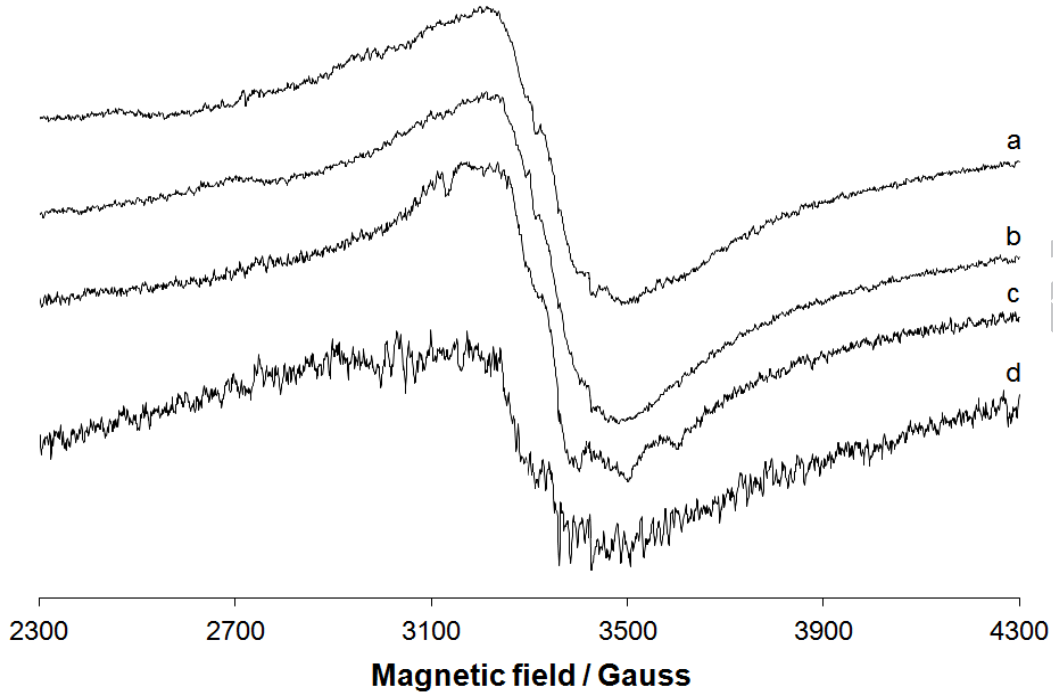

Figure 4. X-band EPR spectra of the complex **1** dissolved in: (a) DMF; (b) DMSO; (c) MeOH) and (d) a mixture CH_2Cl_2/toluene 60/40 v/v.

solution, could suggest that the structure of the complex remains unchanged in an organic solvent, in contrast with other polynuclear metal complexes such as those formed by Cu(II) [51-58].

2.5. Magnetic property

The magnetic properties of compound **1** were studied by variable temperature magnetic susceptibility measurements in the temperature range of 2–300 K in an applied field of 1000 Oe on a powdered microcrystalline sample. The

room-temperature μ_{eff} value is around 4.90μ_B per Mn^{III} ion, which is in good agreement with the expected value for one isolated spin-only Mn^{III} ion (4.90μ_B for g = 2, S = 2). The magnetic behavior of compound **1** is depicted in the form $\chi_M T$ versus T plot (**Figure 5**).

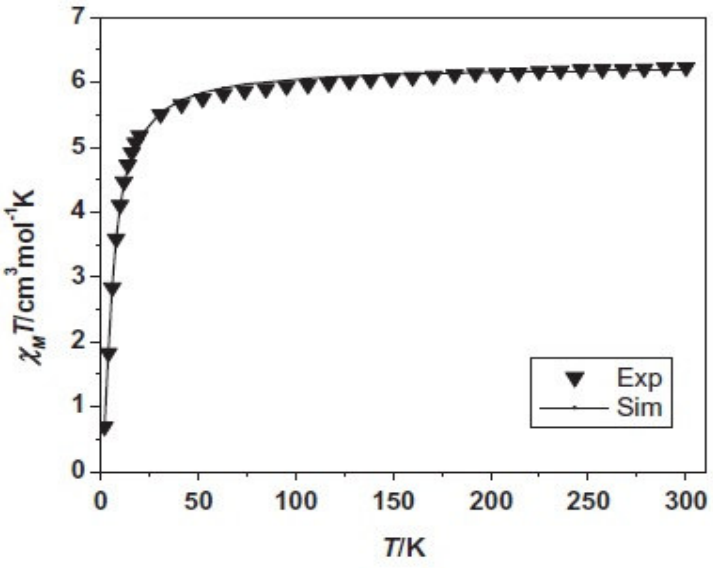

Figure 5. Plot of $\chi_M T$ vs. T for a microcrystalline sample of **1** in 0.1 T.

The temperature dependent $\chi_M T$ data were simulated satisfactorily showing the parameter set of J = -0.602 cm^{-1} with g = 2.043. For compound **1** no satisfactory simulation of the experimental data was possible neglecting any exchange interaction J and taking into account only zero field splitting parameters. The small negative J value is indicative of very weakly antiferromagnetic interactions between the Mn^{III} spin centers [59,60]. Furthermore, comparatively long Mn...Mn distance (5.535 Å in **1**) supports that the super exchange does not arise *via* direct metal–metal exchange [61].

2.6. Redox study

The cyclic voltammetry (CV) experiment was performed using three electrode configurations. The working electrode was a glassy carbon; Pt and Ag wires served as counter and reference electrodes, respectively. **Figure 6** illustrates a typical cyclic voltammogram of 1 mM solution of a complex, in dry acetonitrile using 0.1 M tetra-n-butylammonium hexafluorophosphate [n-Bu_4NPF_6] as supporting electrolyte. The solution was purged by passing a stream of nitrogen gas in the solution for about 10 min, before the measurement. The voltammogram is run between the potentials of + 1.5 and -1.6 V vs. Ag at a scan rate of 100 m V/s. Although the complex was examined not to be electroactive in the high positive (> +1.3 V vs Ag) and negative (< -0.5 V vs Ag) potentials; it undergo redox processes in potential region between +1.2 and-0.2 V vs Ag. A reversible redox couple at -0.14 V *vs* Ag is assigned for Mn^{3+}/Mn^{2+} redox process. A weak irreversible oxidation peaks were also observed at +0.7 V and -1.2 V *vs* Ag. These oxidation peaks could be due to ligand based redox processes.[62] Moreover, weak reversible peak at +1.02 V vs Ag is assigned to be to oxidation of Mn(III) to Mn(IV). The high cathodic and anodic potential difference (about 275 mV) could be due to effect of the complex diffusion rate or an activation barrier from electron transfer process.

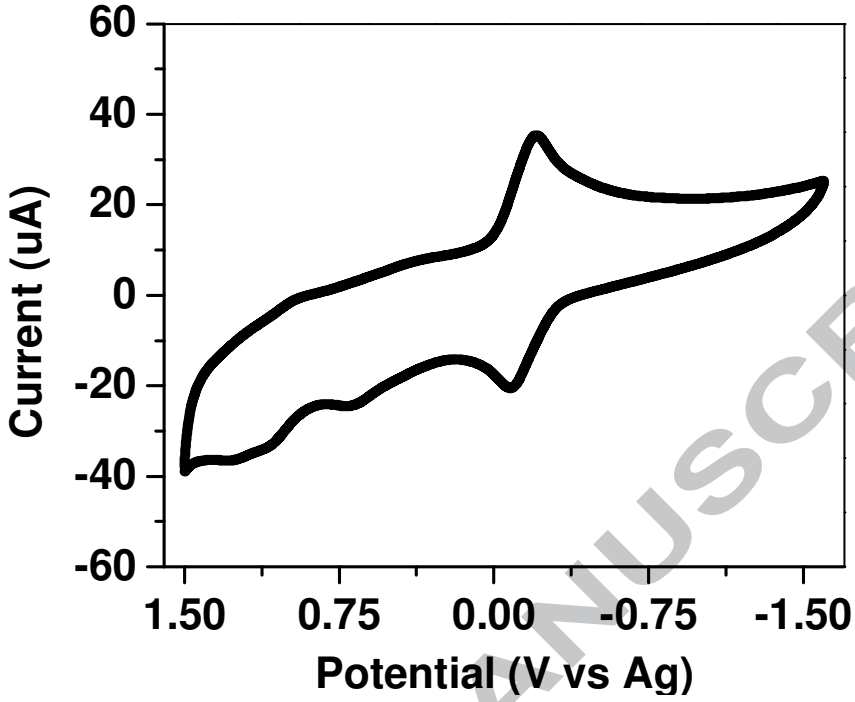

Figure 6. Cyclic voltammetry of 1 mM of complex in 0.1 M Bu_4NPF_6/acetonitrile solution at scan rate of 0.1 V s^{-1} using glassy carbon as working electrode, pt-wire as counter electrode and Ag as reference electrode at room temperature. E_{pc} –cathodic potential and E_{pa} –anodic potential.

2.7. Anti-mycobacterial activity

In the anti-mycobacterial assay, H_2L and complex **1** were tested against *M. tuberculosis* H37Rv ATCC 27294 and *M. tuberculosis* H37Ra ATCC 25177 strains as well as against two clinical strains (strain 1 and strain 2). The results are shown in **Table 2**. *M. tuberculosis* H37Rv and *M. tuberculosis* H37R, well-known indicators,

were used for the drug sensitivity tests. The results showed that both the ligand H_2L and complex **1** both exhibited anti-mycobacterial activity against all the tested M. tuberculosis strains, with MICs of 51.38 µmol/L and MBC values in the range of 51.38-398.71 µmol/L. Both H_2L and complex **1** showed a bactericidal activity and killed the bacteria (**Table 2**). Trias et al, [63] showed that Mycobacterium cheionae developed a pore-forming protein as a mycobacterial porin. On the study of permeability of Mycobacterium smegmatis, Trias & Benz [64] reported that mycobacterial porin formed an important hydrophilic structure where small molecules pass through the pores and diffuse into the cell. In this study, we have evidenced that all compounds show a considerable efficacy on the Mycobacteria strains. The mycobacteria cell wall includes a large amount of complex lipids, lipopolysaccharides and mycolic acids. This constitution makes the cell wall a hydrophobic strong barrier against antimicrobial agents [65,66]. The MIC

Table 2. Antimycobacterial activity (MIC and MBC, µg/ml) of H_2L and **1**.

Compounds	**The minimal inhibitory concentration (MIC)**				**The minimal bactericidal concentration (MBC)**			
	M. tuberculosis RA		*M. tuberculosis* RV		Clinical isolate 1		Clinical isolate 2	
	MIC	MBC	MIC	MBC	MIC	MBC	MIC	MBC
H_2L	51.38	205.59	51.38	205.59	51.38	107.78	51.38	398.71

1	51.38	107.78	51.38	51.38	51.38	51.38	51.38	107.78
Concentrations of antimycobacterial drugs (µmol/L)								
Streptomysin	4.30	8.53	4.30	4.30	2.59	34.29	4.30	-
İzoniazid	3.37	6.81	0.86	6.81	3.37	6.81	3.37	3.37

(Minimal Inhibitory Concentration) and MBC (Minimal Bactericidal Concentration) values are higher in the present case. These data are quite good when compared with known drugs like streptomisin and isoniazid.

2.8. Cell cytotoxicity studies

Figures 7, **8** and **9** show the effects of complex **1** on cell population growth in three human cancer cell lines, human colon carcinoma cells (Caco 2), human breast carcinoma cells (MCF7 cells) and human lung carcinoma cells (A549 cells). To assess the inhibitory effect on the growth of human cancer cells, the cells were cultured for 24 and 48 h with or without the test compound (0-100 µM), and the population growth was determined by MTT assay. In particular, complex **1** shows significant cytotoxic effect on the A549 cell line (**Figure 9**); additionally, **1** also exhibits good cytotoxic activity against MCF7 cancer cell lines (**Figure 8**). When this result is compared with the control group, it can be seen that a time-dependent decrease on mitochondrial activity for all concentrations occurs. The manganese complex shows a

cytotoxic effect which induces DNA hypermetilation and oxidative stress on the cancer cell lines. Moreover, the 50% inhibitory concentration (IC_{50}) as determined by MTT assay after 48 h of incubation shows the highest activity with an IC_{50} value of 46.00 ± 1.09 μM.

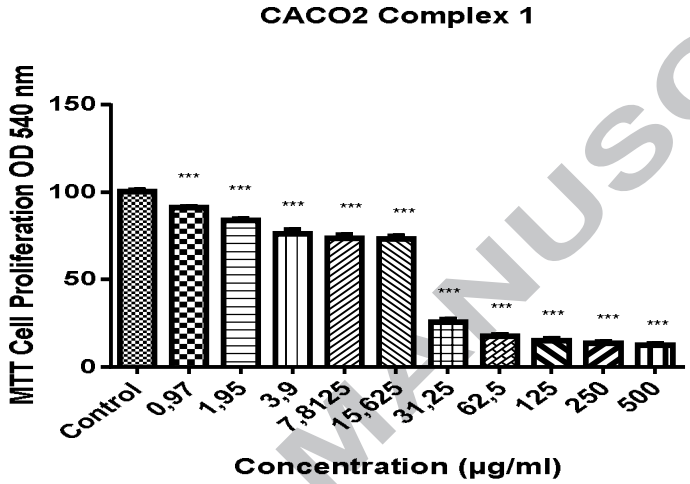

Figure 7. Cytotoxic effects of complex **1** on CACO2 cell line.

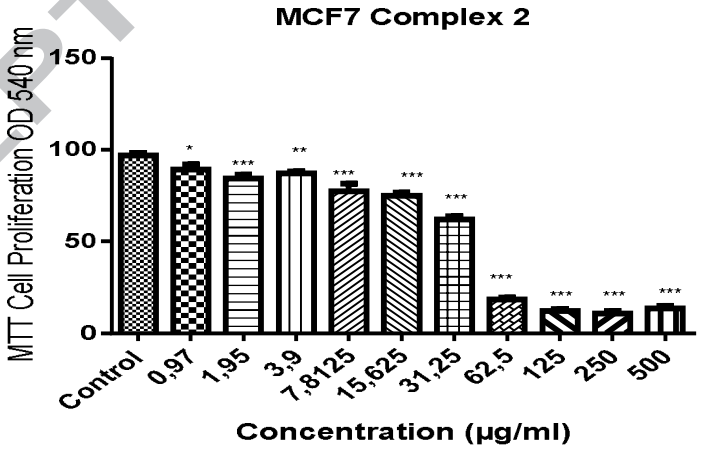

Figure 8. Cytotoxic effects of complex **1** on MCF7 cell line.

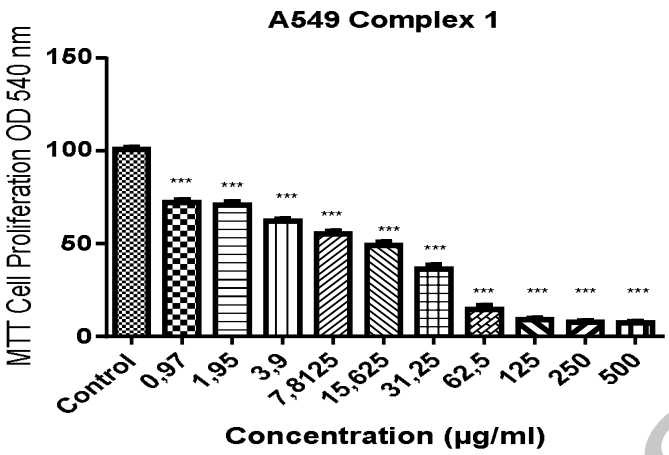

Figure 9. Cytotoxic effects of complex **1** on A549 cell line.

3. Experimental section

3.1. Materials

All chemicals and solvents used for the synthesis were of reagent grade, obtained commercially and used as received. Salicyldehyde and ethylenediamine were purchased from Aldrich Chemicals. Hydrated manganese(II) trichloroacetate was prepared by the treatment of basic manganese(II) carbonate, $MnCO_3.Mn(OH)_2$ (AR grade, E. Merck), with 60% trichloroacetic acid (AR grade, E. Merck), followed by slow evaporation on a steam bath. It was then filtered through a fine glass frit and stored in a $CaCl_2$ desiccators.

3.2. Physical techniques

Microanalytical data (C, H, and N) were collected on a Perkin–Elmer 2400 CHNS/O

elemental analyzer. FTIR spectra were recorded on a Perkin-Elmer RX-1 spectrophotometer in the range 4000–400 cm^{-1} as KBr pellets. Electronic spectra were measured on a Lambda 25 (U.V.–Vis.–N.I.R.) spectrophotometer. EPR spectra were recorded from 0 to 8000 Gauss in the temperature range 77-298 K with an X-band (9.4 GHz) Bruker EMX spectrometer equipped with an HP 53150A microwave frequency counter. Magnetic properties were investigated with a Quantum Design MPMS-XL superconducting quantum interference device magnetometer (SQUID) at an applied field 0.5 T in a temperature range 5-300 K. The diamagnetic correction was carried out by using Pascal constants.

3.3. Synthesis of $\{[C_6H_4(O)CHN(CH_2)_2NCH(O)C_6H_4]Mn(N_3)\}_n$ (***1***)

To a methanol solution (10 mL) of $Mn(CCl_3COO)_2.4H_2O$ (0.716 g, 2 mmol), the ligand H_2L [43] (2 mmol) in 15 mL of methanol was added with under constant stirring. The resulting green solution was kept boiling for 10 mins. After that an aqueous solution (10 mL) of anhydrous NaN_3 (0.195 g, 3 mmol) was added slowly in warm condition and the mixture was kept undisturbed at room temperature. Dark-brown square-shaped single crystals of **1** were generated after one week. These were separated over filtration and air-dried before X-ray diffraction analysis. Yield: 0.58 g. Anal. Calc. for $C_{16}H_{14}MnN_5O_2$: C, 52.86; H, 3.88; N, 19.27. Found: C, 52.59;

H, 4.12; N, 19.41%.

3.4. X-ray crystallography

The crystal structure of compound **1** was determined by X-ray diffraction methods. Intensity data and cell parameters were recorded at 190(2) K on a Bruker APEX II equipped with a CCD area detector and a graphite monochromator (MoKα radiation λ = 0.71069 Å) The raw frame data were processed using SAINT and SADABS to yield the reflection data file [67]. The structure was solved by Direct Methods using the SIR97 program [68] and refined on F_o^2 by full-matrix least-squares procedures, using the SHELXL-2014/7 program [69] in the WinGX suite v.2014.1 [70]. All non-hydrogen atoms were refined with anisotropic atomic displacements. The hydrogen atoms were included in the refinement at idealized geometry (C-H 0.95 Å) and refined "riding" on the corresponding parent atoms. The weighting scheme used in the last cycle of refinement was $w = 1/ [\sigma^2 F_o^2 + (0.0523P)^2]$, where $P = (F_o^2 + 2F_c^2)/3$. Geometric calculations were performed with the PARST97 program [71]. Crystal data and experimental details for data collection and structure refinement are reported in **Table 3**. Crystallographic data for the structures reported have been deposited with the Cambridge Crystallographic Data Centre as supplementary publication no. CCDC-1501177 and can be obtained free of charge on application to

the CCDC, 12 Union Road, Cambridge, CB2 1EZ, UK (fax: +44-1223-336-033; e-mail deposit@ccdc.cam.ac.uk or http://www.ccdc.cam.ac.uk).

Table 3. Crystal data and structure refinement information for **1**.

Compound	**1**
empirical formula	$C_{16}H_{14}N_5O_2Mn$
M	363.26
crys syst	Orthorhombic
space group	*Pca2₁*
a/Å	10.881(3)
b/Å	11.070(3
c/Å	12.943(3)
V/Å^3	1559.0(7)
Z	4
T/K	190(2)
ρ /g cm^{-3}	1.548
μ /mm^{-1}	0.866
F(000)	744
total reflections	12235
unique reflections (R_{int})	2861 (0.0866)
observed reflections $[F_o>4\sigma(F_o)]$	2055
GOF on F^{2a}	1.010
$R_{indices}$ $[F_o>4\sigma(F_o)]^b R_1$, wR_2	0.0464, 0.0977
largest diff. peak and hole (eÅ^{-3})	0.519, -0.374

[a]Goodness-of-fit S = $[\Sigma w(F_o^2-F_c^2)^2/ (n-p)]1/2$, where n is the number of reflections

and p the number of parameters. [b]$R_1 = \Sigma \| F_o | - | F_c \| / \Sigma | F_o |$, $wR_2 = [\Sigma[w(F_o^2-F_c^2)^2]/\Sigma[w(F_o^2)^2]]^{1/2}$.

3.5. Anti-mycobacterial activity

3.5.1. Medium

In the assays, Mycobacteria Growth Indicator Tubes (MGIT) and their supplements, BBL MGIT OADC enrichment and BBL MGIT PANTA were purchased from BD. The MGIT Mycobacteria Growth Indicator Tube contains 4 mL of modified Middlebrook 7H9 Broth base.

3.5.2. Inoculum preparation

For the cultivation of mycobacteria, the MGIT (Mycobacteria Growth Indicator Tube), a fluorescent compound is embedded in silicone on the bottom, then 4 mL of modified Middle brook 7H9 Broth base are added to the mixture. After that 0.5 mL of OADC enrichment, (an oleic acid, albumin, dextrose and catalase) and PANTA antibiotic mixture to prevent the growth of any non-mycobacteria (0.1 mL) are added to this medium. Oleic acid plays an important role in metabolism of mycobacteria; Albumin acts as a protective agent; Dextrose is an energy source; Catalase destroys toxic peroxides. Tubes are incubated at 37 °C. For positive control, MGIT tubes are prepared by inoculating bacteria. An un-inoculated MGIT tube is used as a negative

control. Blood Agar is used for checking the growth of other bacteria. Daily tube reading starts on the second day of incubation using a Micro MGIT fluorescence reader which has a long wave UV light [72]. To prepare inoculums from a positive BACTEC MGIT tube, the positive tubes (day 1 or day 2 positive) are used directly as inoculums. The positive tubes between day 3 and day 5 are diluted to 1:4 ratio by sterile saline. Inoculums, prepared from a Day 1 to Day 5 MGIT 7 mL positive tube, range between 0.8×10^5 and 3.2×10^5 CFU/mL. Each assay is performed according to the MGIT manual fluorometric susceptibility test procedure recommended by the manufacturer [72,73].

3.5.3. Antimycobacterial susceptibility assay

The activity of the ligand, H_2L and complex **1** against M. tuberculosis strains was tested using the Microplate Presto Blue Assay (MPBA) by the method described by Collins & Franzblau [74] and modified by Jimenez-Arellanes et al. [75] 128 µl of compound **1** and 72 µl of 7H9 broth were transferred in the first column; then 100 µl of 7H9 broth was transferred from column 2 to column 8. Column 9 and 10 were the positive and negative control, respectively. 100 µl of a mixture of broth and of compound **1** were transferred from column 1 to column 2, then mixed by pipettes three times; the procedure was repeated to provide serial 1:2 dilutions. 100 µl of the

excess medium was discarded from the wells in column 8. Afterwards, 20 µl of *M. tuberculosis* inoculum was added to the wells of column 1 to 8 and to the positive control columns. Negative control columns were not inoculated with bacteria. Positive control columns included 7H9 broth and bacteria, while negative control columns contained 7H9 broth and compound **1**. Final-test concentration ranges were 423.68-6.62 µmol/L in the mixture. Microplates were inoculated with the bacterial suspension (20 µL per well) except for the negative control and incubated at 37 °C for 6 days. Presto blue (15 µL, Life Technologies) was then added to the bacterial growth control wells (without compound **1**) and the microplates were incubated at 37 °C for an additional 24 h. If the dye turned from blue to pink (indicating positive bacterial growth), the Presto blue solution was added to the other wells to determine the MIC values. All tests were performed in triplicate. The minimal inhibitory concentration (MIC) was defined as the lowest concentration of sample that prevents a color change to pink. The minimal bactericidal concentration (MBC) corresponded to the minimum compound concentration which does not cause a color change in the cultures when re-incubated in fresh medium [76,77]. Streptomycin (STR) from Sigma, and isoniazid (INH) from Fluka were used as standard drugs.

3.6. Cell cytotoxicity

3.6.1. Cell culture

A549 (non-small cell lung cancer), MCF-7 (breast cancer) and Caco-2 (colon cancer cell line) were used in the study, provided by ATCC cell bank. The cells were grown in RPMI 1640 medium supplemented with 2 mM L-glutamine and 10% fetal bovine serum, 1% penicillin-streptomycin at a temperature of 37 ^{o}C in a humidified incubator with a 5% CO_2 atmosphere.

3.6.2. MTT assay

Complexes **1** and **2** having the concentration of 1500, 250, 125, 62.5, 31.25, 15.625, 7.812, 3.9, 1.95, 0.97 µg/ml were seeded in 5×10^3 cells which were cultivated in each well of a 96-well plate. After 24 hours of incubation, 0.1 mL of WST-1 working solution was added to each well and they were incubated at 37 °C in a 5 % CO_2 incubator for 3-4 hours. The absorbance intensity of the living cell in the plate was read in an ELISA device (Cytation3, Biotek, USA) at 450 nm. The acquired absorbance values corresponded to the metabolic activities of the cells in the culture. Because this value was correlated to the number of living cells, the results were expressed in liveliness percent and calculated using the formula below.

$$Liveliness\ percent = \frac{100}{Absorbance\ of\ the\ control / Absorbance\ of\ the\ sample}$$

4. Conclusion

A new Schiff base assisted, Mn(III) one-dimensional network was generated and spectroscopically characterized. The solid state structure of **1** shows that the Mn atoms in the polymer present a distorted octahedral arrangement. Solvent-mediated EPR spectra is carried out and found to remain unchanged while varying from coordinating to non-coordinating organic solvents. The temperature dependent magnetic moment supports the presence of weak antiferromagnetic interactions between the bridging Mn(III) ions. Both the ligand H_2L and complex **1** exhibit anti-mycobacterial activity and considerable efficacy on *M. tuberculosis* H37Rv ATCC 27294 and *M. tuberculosis* H37Ra ATCC 25177 strains. Further investigations in this area with other transition metal ions and chemo-sensor activities of the ligand for selective detection of metal ions are currently being carried out in our laboratories.

Appendix A. Supplementary data

CCDC 1501177contains the supplementary crystallographic data for complex **1**. These data can be obtained free of charge via http://www.ccdc.cam.ac.uk/conts/retrieving.html, or from the Cambridge Crystallographic Data Centre, 12 Union Road, Cambridge CB2 1EZ, UK; fax: (+44) 1223-336-033; or e-mail: deposit@ccdc.cam.ac.uk.

Acknowledgements

KD and CS would like to thank DST (Department of Science and Technology, New Delhi, India) for the grant (SR/S1/IC-31/2008) to carry out the present study.

References

[1] R. Ziessel, Coord. Chem. Rev. 216 (2001) 195-223.

[2] M. Albrecht, Chem. Rev. 101 (2001) 3457-3498.

[3] S. Chandra, X. Sangeetika, Spectrochim. Acta A 60 (2004) 147-153.

[4] E. Fujita, B. S. Brunschwig, T. Ogata, S. Yanagida, Coord. Chem. Rev. 132 (1994) 195-200.

[5] E. Kimura, S. Wada, M. Shiyonoya, Y. Okazaki, Inorg. Chem. 33 (1994) 770-778.

[6] B. De Clercq, F. Verpoort, Macromolecules 35 (2002) 8943-8947.

[7] T. Opstal, F. Verpoort, *Angew. Chem. Int. Ed. Engl.*, 2003, **42**, 2876-2879.

[8] S. L. Lambert, C. L. Spiro, R. R. Gagne, D. A. N. Hendriekson, Inorg. Chem. 21 (1982) 68-72.

[9] Y. Y. Chen, D. E. Chu, B. D. McKinney, L. J. Willis, S. E. Cummings, Inorg. Chem. 20 (1981) 1885-1892.

[10] J. Ribas, M. Monfort, I. Resino, X. Solans, P. Rabu, F. Maingot, M. Drillan, Angew. Chem., Int. Ed. Engl. 35 (1996) 2520-2526.

[11] R. Vicente, A. Escuer, E. Penalba, X. Solans, M. Font-Badia, J. Chem. Soc., Dalton Trans. (1994) 3005-3008.

[12] R. Vicente, A. Escuer, J. Ribas, X. Solans, J. Chem. Soc., Dalton Trans. (1994) 259-262.

[13]J. Ribas, C. Diaz, X. Solans, M. Font-Bardia, J. Chem. Soc., Dalton Trans. (1997) 35-38.

[14] H. Miyasaka, R. Clerac, T. Ishii, H.-C. Chang, S. Kitagawa, M. Yamashita, J. Chem. Soc., Dalton Trans. (2002) 1528-1534.

[15] O. Kahn, Molecular Magnetism, VCH, Weinheim, Germany, 1993.

[16] J. S. Miller, A. J. Epstein, Angew. Chem. Int. ed. Engl. 33 (1994) 385-416.

[17] M. Verdaguer, A. Bleuzen, V. Marvaud, J. Vaissermann, M. Seuleiman, C. Desplanches, A. Scuiller, C. Train, R. Garde, G. Gelly, C. Lomenech, I. Rosenman, P. Veillet, C. Cartier, F. Villain, Coord. Chem. Rev. 190-192 (1999) 1023-1047.

[18] C. Mathoniere, J. -P. Sutter, J. V. Yakhmi, in: J.S. Miller, M. Drillon (Eds.), Magnetism: Molecules to Materials, vol. 4, VCH, Weinheim, 2002, pp. 1-40.

[19] C. E. Hulme, M. Watkinson, M. Haynes, R. G. Pritchard, C. A. McAuliffe, N.

Jaiboon, B. Beagley, A. Sousa, M. R. Bermejo, M. Fondo, J. Chem. Soc., Dalton Trans. (1997) 1805-1814.

[20] N. Matsumoto, Z. J. Zhong, H. Okawa, S. Kida, Inorg. Chim. Acta 160 (1989) 153-157.

[21] N. Matsumoto, N. Takemoto, A. Ohyosi, H. Okawa, Bull. Chem. Soc. Jpn. 61 (1988) 2984-2986.

[22] M. R. Bermejo, A. Castineiras, J. C. Garcia-Monteagudo, M. Rey, A. Sousa, M. Watkinson, C. A. McAuliffe, R. G. Pritchard, R. L. Beddoes, J. Chem. Soc., Dalton Trans. (1996) 2935-2944.

[23] A. Garcia-Deibe, A. Sousa, M. R. Bermejo, P. P. MacRory, C. A. McAuliffe, R. G. Pritchard, M. Helliwell, J. Chem. Soc., Chem Commun. (1991) 728-729.

[24] H. Miyasaka, N. Matsumoto, H. Okawa, N. Re, E. Gallo, C. Floriani, J. Am. Chem. Soc. 118 (1996) 981-994.

[25] Y. Sato, H. Miyasaka, N. Matsumoto, H. Okawa, Inorg. Chim. Acta 247 (1996) 57-63.

[26] N. Matsumoto, H. Okawa, S. Kida, T. Ogawa, A. Ohyoshi, Bull. Chem. Soc. Jpn. 62 (1989) 3812-3817.

[27] H. -L. Shyu, H.-H. Wie, Y. Wang, Inorg. Chim. Acta 290 (1999) 8-14.

[28] A. Das, G. M. Rosair, M. S. El Fallah, J. Ribas, S. Mitra, *Inorg. Chem*. 2006, **45**,

3301-3306;

[29] S. K. Dey, N. Mondal, R. Vicente, M. S. El Fallah, A. Escuer, X. Solans, M. FontBardía, T. Matshusita, V. Gramlich, S. Mitra, Inorg. Chem. 43 (2004) 2427-2434.

[30] R. Cortés, M. K. Urtiaga, L. Lezama, J.L. Pizarro, M. I. Arriortua, T. F. Rojo, Inorg. Chem. 36 (1997) 5016-5021.

[31] R. Cortes, T. I. Ruiz de Larramendi, L. Lezama, T. Rojo, K. Urtiaga, M. I. Arriortua, J. Chem. Soc., Dalton Trans. (1992) 2723-2729.

[32] M. I. Arriortua, R. Cortes, L. Lezama, T. Rojo, X. Solans, M. Font-Bardía, Inorg. Chim. Acta 174 (1990) 263-269.

[33] M. D. Duggan, D. N. Hendrickson, Inorg. Chem. 13 (1974) 2929-2936.

[34] T. Rojo, R. Cortes, L. Lezama, I. M. Arriortua, G. Villenueve, J. Chem. Soc., Dalton Trans. (1991) 1779-1783.

[35] C. G. Pierpont, D. N. Hendrickson, D. M. Duggan, F. Wagner, E. K. Barefield, R. L. Martin, Inorg. Chem. 14 (1975) 604-610.

[36] P. Chaudhuri, M. Gottmann, D. Ventur, K. Wieghardt, B. Nuber, J. Weiss, J. Chem. Soc., Chem. Commun. (1985) 1618-1619.

[37] J. Ribas, A. Escuer, M. Monfort, R. Vicente, R. Cortés, L. Lezama, T. Rojo, Coord. Chem. Rev. 193 (1999) 1027-1068.

[38] E. Ruiz, J. Cano, S. Alvarez, P. Alemany, J. Am. Chem. Soc. 43 (1998) 120-121.

[39] A. L. Okunade, M. P. F. Elvin-Lewis, Phytochem. 65 (2004) 1017-1022.

[40] N. Lall, M. D. Sarma, B. Hazra, J. J. Meyer, J. Antimicro. Chemo. 51 (2003) 435-438.

[41] E. Banfi, M. G. Mamolo, D. Zampieri, L. Vio, C. M. Bragadin, J. Antimicro. Chem. 48 (2001) 705-711.

[42] V. Jarlier, H. Nikaido, Microbiol. Lett. 123 (1994) 11-18.

[43] C. Floriani, F Calderazzo, J. Chem. Soc. A (1971) 3665-3669.

[44] T. Gupta, M. K. Saha, S. Sen, S. Mitra, A, J. Edwards, W. Clegg, Polyhedron 18 (1999) 197-201.

[45] K. Nakamoto, Infrared and Raman Spectra of Inorganic and Coordination Compounds, Part B: Applications in Coordination, Organometallic and Bioinorganic Chmemistry, 5th Edition , A Wiley-Interscience Publication John Wiley & Sons Inc., New York, 1997, pp. 124-126].

[46] A. B. P. Lever, Inorganic Electronic Spectroscopy, second ed., Elsevier, New York, 1984.

[47] A.-L. Barra, D. Gatteschi, R. Sessoli, G. L. Abbati, A. Cornia, A. C. Fabretti, M. G. Uytterhoeven, Angew. Chem. Int. Ed. Engl. 36 (1997) 2329-2331.

[48] A. C. Rizzi, N. I. Neuman, P. J. González, C. D. Brondino, Eur. J. Inorg. Chem.

(2016) 192-207.

[49] G. H. Reed, R. R. Poyner, In *Metal* ions in biological systems, H. Sigel, A. Sigel, Eds. Marcel Dekker: New York, 2000; Vol. 37, pp 183-207.

[50] G. H. Reed, G. D. Markham, In Biological Magnetic Resonance, L. J. Berliner, J. Reuben, Eds. Plenum Press: New York, 1984; Vol. 6, pp 73-142.

[51] W. A. Alves, R. H. de Almeida Santos, A. Paduan-Filho, C. C. Becerra, A. C. Borin, A. M. Da Costa Ferriera, Inorg. Chim. Acta 357 (2004) 2269-2278.

[52] M. A. Ali, A. H. Mirza, R. J. Fereday, R. J. Butcher, J. M. Fuller, S. C. Drew, L. R. Gahan, G. R. Hanson, B. Moubaraki, K. S. Murray, Inorg. Chim. Acta 358 (2005) 3937-3948.

[53] I. A. Koval, M. Sgobba, M. Huisman, M. Lüken, E. Saint-Aman, P. Gamez, B. Krebs, J. Reedijk, Inorg. Chim. Acta 359 (2006) 4071-4078.

[54] C. P. Pradeep, S. K. Das, Polyhedron 28 (2009) 630-636.

[55] S. Thakurta, C. Rizzoli, R. J. Butcher, C. J. Gómez-García, E. Garribba, S. Mitra, Inorg. Chim. Acta 363 (2010) 1395-1403.

[56] A. Ray, S. Mitra, A. D. Khalaji, C. Atmani, N. Cosquer, S. Triki, J. M. Clemente-Juan, S. Cardona-Serra, C. J. Gomez-Garcia, R. J. Butcher, E. Garribba, D. Xu, Inorg. Chim. Acta 363 (2010) 3580-3588.

[57] S. Shit, M. Nandy, G. Rosair, M. Salah El Fallah, J. Ribas, E. Garribba, S.

Mitra, Polyhedron 52 (2013) 963-969.

[58] S. Saha, A. Sasmal, C. R. Choudhury, C. J. Gomez-Garcia, E. Garribba, S. Mitra, Polyhedron 69 (2014) 262-269.

[59] M. Soler, P. Artus, K. Folting, J. C. Huffman, D.N. Hendrickson, G. Christou, Inorg. Chem. 40 (2001) 4902-4912.

[60] C. Boskovic, M. Pink, J. C. Huffman, D.N. Hendrickson, G. J. Christou, J. Am. Chem. Soc. 123 (2001) 9914-9915.

[61] R. L. Martin, in: E. V. Ebsworth, A. Maddock, A.G. Sharp (Eds.), New Pathways in Inorganic Chemistry, Cambridge University Press, Cambridge, 1968, p. 175.

[62] S. Hotchandani, U. Ozdemir, C. Nasr, S. I. Allakhverdiev, N. Karacan, V. V. Klimov, P. V. Kamat, R. Carpentier, Bio-electrochem. & Bio-energetics 48, (1999) 53-59.

[63] J. Trias, V. Jarlier, R. Benz, Science 258 (1992) 1479-1481.

[64] J. Trias, R. Benz, Mol. Microbio. 14 (1994) 283-286.

[65] D. E. Minnikin, M. Goodfellow, in microbiological classification and identification; R.G. Board, Eds.; Academic: London, 1980; p 189.

[66] D. E. Minnikin, Lipids; complex lipids, their chemistry, biosynthesis and roles. In the biology of mycobacteria. C. Ratledge and J. Stanford, Eds.; London;

Academic Press, Inc., 1982, p 95.

[67] SADABS Bruker AXS; Madison, Wisconsin, USA, 2004; SAINT, *Software Users Guide*, *Version 6.0*; Bruker Analytical X-ray Systems, Madison, WI (1999). G. M. Sheldrick, SADABS v2.03: *Area-Detector Absorption Correction*. University of Göttingen, Germany (1999).

[68] A. Altomare, J. Appl. Cryst. 32 (1999) 115-119.

[69] G. M. Sheldrick, Acta Crystallogr. A64 (2008) 112-122.

[70] (a) L. J. Farrugia, J. Appl. Crystallogr. 45 (2012) 849-854; (b) P. v.d. Sluis, A. L. Spek, Acta Cryst., Sect A. 46 (1990) 194-201.

[71] M. Nardelli, J. Appl. Crystallogr. 29 (1996) 296-300.

[72] B. D. Becton, Dickinson and Company Newsletter BD Bactec MGIT 960 SIRE kit now FDA-cleared for susceptibility testing of Mycobacterium tuberculosis. Microbiology News & Ideas 13: 4-4, 2002.

[73] NCCLS, (2003). National Committee for Clinical Laboratory Standards (NCCLS). Susceptibility Testing of Mycobacteria, Nocardiae, and Other Aerobic Actinomycetes; Approved Standard. NCCLS document M24-A [ISBN 1-56238-500-3]. NCCLS, 940 West Valley Road, Suite 1400, Wayne, Pennsylvania 19087-1898 USA, 2003.

[74] L. Collins, S. G. Franzblau, Antimicro. Agents Chemother. 41 (1997) 1004-1009.

[75] A. Jimenez-Arellanes, M. Meckes, R. Ramirez, J. Torres, J. Luna-Herrera,

Phytother. Res. 17 (2003) 903-908.

[76] G. R. Battu, B. M. Kumar, Willd. Pharmacognosy J. 2 (2010) 456-463.

[77] P. Bontempo, V. Carafa, R. Grassi, A. Basile, G. C. Tenore, C. Formisano, D. Rigano, L. Altucci, Food Chem. Toxicology (2013) 304-312.

A zig-zag end-to-end azido bridged Mn^{III} 1-D coordination polymer: Spectral elucidation, magnetism, redox study and biological activity

Kuheli Das[a,b], Amitabha Datta[a,b,*], Belete B. Beyene[a], Chiara Massera[c], Eugenio Garribba[d], Chittaranjan Sinha[b,*], Takashiro Akitsu[e], Shinnosuke Tanka[e]

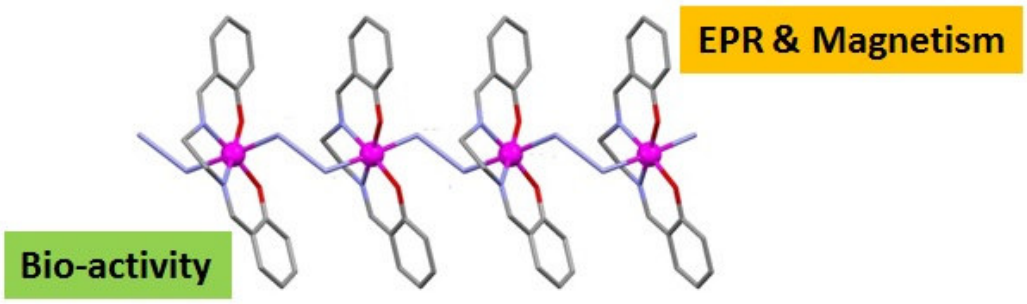

A zig-zag end-to-end azido bridged Mn^{III} 1-D coordination polymer: Spectral elucidation, magnetism, redox study and biological activity

Kuheli Das[a,b], Amitabha Datta[a,b,*], Belete B. Beyene[a], Chiara Massera[c], Eugenio Garribba[d], Chittaranjan Sinha[b,*], Takashiro Akitsu[e], Shinnosuke Tanka[e]

A Mn(III) 1-D coordination polymer is generated as systematically characterized by different spectral analysis. The magnetic and cyclic voltammetric studies are also governed. Both the ligand and complex exhibit anti-mycobacterial activity and considerable efficacy on different tuberculosis cell lines. The cytotoxicity study on human cancer cell lines (Caco 2, MCF7 and A549) are also presented.